Anal. Methods Environ. Chem. J. 6 (4) (2023) 5-18

AMECJ

Research Article, Issue 4
Analytical Methods in Environmental Chemistry Journal
Journal home page: www.amecj.com/ir

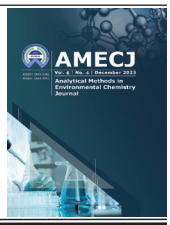

Surface-engineered TiO_2 nanoparticles incorporated Chitosan polymer membrane for seawater desalination: Fabrication, characterization, and performance evaluation

Muhammad Nurdin [a,*], Mike Delvinasari [a], La Ode Ahmad [a], Maulidiyah Maulidiyah [a], Dwiprayogo Wibowo[b,c], Faizal Mustapa [d], Amir Mahmud [e], Muhammad Idris [f], and Muh. Ramli [h]

[a] *Department of Chemistry, Faculty of Mathematics and Natural Sciences, Universitas Halu Oleo, Kendari 93231, Southeast Sulawesi, Indonesia.*
[b] *Department of Environmental Science, School of Environmental Science, Universitas Indonesia, Jakarta 10430, Indonesia.*
[c] *Department of Environmental Engineering, Faculty of Engineering, Universitas Muhammadiyah Kendari, Kendari 93231, Southeast Sulawesi, Indonesia.*
[d] *Department of Marine Sciences, Institut Teknologi dan Bisnis Muhammadiyah Kolaka, Kolaka 93511, Southeast Sulawesi, Indonesia.*
[e] *Department of Fishery Resources, Faculty of Marine, Universitas Muhammadiyah Kendari, Kendari 93231, Southeast Sulawesi, Indonesia.*
[f] *Department of Agriculture Sciences, Faculty of Agriculture, Universitas Halu Oleo, Kendari 93231, Southeast Sulawesi, Indonesia.*
[h] *Department of Marine Sciences, Faculty of Marine, Universitas Halu Oleo, Kendari 93231,Southeast Sulawesi, Indonesia.*

ARTICLE INFO:

Received 17 Jul 2023
Revised form 23 Sep 2023
Accepted 10 Nov 2023
Available online 28 Dec 2023

Keywords:
Desalination,
Membrane,
TiO_2,
Polymer structure,
Reverse Osmosis,
Seawater,

ABSTRACT

The effect of surface coating over titanium dioxide nanoparticles (TiO_2-NPs) incorporated with chitosan (TiO_2-NPs/chitosan) was evaluated as a reverse osmosis membrane (RO) for enhanced performance on seawater desalination. The impact of surface coating on the chitosan membrane performance in seawater reverse osmosis (SWRO) was investigated by altering the mass of TiO_2-NPs (0.25 g and 0.5 g) used for the surface coating RO membrane. TiO_2-NPs were applied to the membranes using a surface coating technique and dried to create a sturdy polymer structure. The characteristic of fabricated membranes shows the function group reflects on organic compounds from /chitosan membranes polymer (–OH, -CH, C=O, C-O-C, $-CH_3$, C-O, and NH_2). In addition, TiO_2-NPs are expressed in the wavenumber range of 850-500 cm^{-1}, which characterizes the presence of Ti-O-Ti bonds. Morphological and crystal analyses of TiO_2-NPs incorporated in chitosan membrane show significantly smaller pores formed because TiO_2-NPs are essential in the high permeability performance under the amorphous phase structure. Also, the high performance of fabricated membranes was evaluated against water flux and salt. Adding TiO_2-NPs can decrease the water flux value by 23 L m^{-2} h^{-1} and increase salt rejection by 52.94%. In optimized pH, the seawater desalination had efficient recovery.

1. Introduction

Indonesia's marine waters cover 70% of its total land area, making it an excellent opportunity to increase the utilization of seawater as raw water as a source of clean water that can be used to meet the needs of the people in Indonesia [1, 2]. Therefore, seawater treatment is needed to remove or reduce its salt content using RO desalination techniques to become clean water. Pure water is a vital element

*Corresponding Author: Muhammad Nurdin
Email: mnurdin06@gmail.com
https://doi.org/10.24200/amecj.v6.i04.246

within the ecosystem, playing a crucial role in the advancement and well-being of humans and various other forms of life [3,4]. The increase in population has led to a situation where not every segment of society can access uncontaminated water. [5]. As a result, many people utilize groundwater and river water for domestic purposes, even though the water is not necessarily suitable for consumption [6]. However, even though the potential availability of water is relatively abundant, people often experience difficulties accessing and fulfilling their water needs for daily life. These problems have led to a lot of research on seawater purification processes. One of the most widely used methods is using semipermeable membranes in RO desalination, which separates low molecular weight solutes such as inorganic salts or small organic molecules such as glucose and sucrose from the solution [7]. RO membranes are widely utilized in various filtration processes, such as groundwater filtration, seawater, and brackish water desalination [8]. The RO process requires membranes to filter out salt molecules to produce ready-to-use fresh water [9]. Transporting specific ions and removing different ions use porous media or membranes. These semi-porous membranes serve as barriers that divide molecules by their respective sizes in a solution. Among the various methods involving membranes for separation, there's the ultrafiltration technique, which relies on pressure differentials for the separation process. The elements isolated within a liquid are contingent on the size and composition of the dissolved substances. [10,11]. Ultrafiltration membranes are principally used to retain colloids and macromolecules but pass salt particles. Separation using membranes was chosen due to its simple, energy-efficient, and environmentally friendly process. Ultrafiltration membranes are usually made of polymeric materials; one of the most commonly used is cellulose acetate (CA) compound [12,13]. RO membranes can be made from various materials; one uses CA compound, which has advantages as an easy-to-produce and renewable raw material source. The disadvantages of the CA membrane are that it is susceptible to acidic and base solutions and is easy for natural microbes [14,15]. The selection of polymers as membrane materials is based on structural factors that will affect the intrinsic properties of the polymer, namely perm selectivity [16]. However, it seems that the CA compound has a full role in the basic ingredients of polymer membrane formation. It dissolves easily with acetone solution and has high capabilities in the ultrafiltration process and high selectivity to filter small materials [17]. The CA compound cannot stand alone as a polymer membrane component; it requires a reinforcing additive compound to improve the membrane's resistant characteristics under stressed conditions. In addition, the function of additive compounds has a role in influencing the formation of membrane morphology, both physicochemical to produce high-performance material properties. PEG is one of the organic compound additives that can reliably improve polymer membrane properties such as surface porosity and membrane pore distribution [18,19]. In some studies, adding PEG as an additive improves membrane performance, like enlarging membrane pores while maintaining membrane resistance to external factors. Besides, the basic membrane organic using CA and PEG is a potential material when combined with chitosan [20]. It has an excellent ability as a coagulant material because it contains many amine groups ($-NH_2$) that are beneficial in the polymetric system of membrane manufacturing. The presence of amine and hydroxyl groups in chitosan makes it have polycationic properties to increase the coagulant in membrane formation, thus strengthening membrane stiffness and high durability in water treatment [21]. These groups can be evaluated with instruments such as Fourier-transform infrared spectroscopy (FTIR) to identify the infrared spectrum of the absorption or emission of the synthesized RO membrane. This characterizes the chemical groups that play a role in membrane formation and influence the adsorption performance. Amine groups in the membrane play a role in various adsorption reaction mechanisms with metal ions. In addition, the amine groups on chitosan are easily modified to improve the

adsorption ability and sorbent to handle metal ions in wastewater. In addition, the synthesized membrane observed the crystallinity and morphology to describe the properties of the membranes analyzed using XRD and SEM instrumentation. They are commonly used in material analysis to observe the porosity and stiffness of the membrane.

In this study, we varied the addition of TiO_2 material as a photocatalyst and antifouling agent because it is believed to be a bioceramic material that is resistant in various conditions with non-toxic, antimicrobial, and environmentally friendly properties, making it safe to use as a base material for making membranes with high strength [22,23]. Amazingly, it is widely used as a water purifier under photocatalyst performance for demineralizing organic, inorganic, and microorganisms dissolved in wastewater. In some of our recent research, TiO_2 is applied as an antibacterial material in inhibiting bacterial growth [24], a photocatalyst material for treating organic pollutants in wastewater, and an electrochemical sensor for detecting organic pollution in wastewater because it has high photoactivity and chemical stability, making it resistant to photo corrosion under neutral solution conditions [25,26]. In addition, it also has redox properties that can oxidize organic pollutants and reduce the number of metal ions in water. This study discovered the unique effect of chitosan semipermeable membrane incorporating TiO_2-NPs. The mass variation of TiO_2 was shown to significantly influence the characterization and performance test of the fabricated membranes under RO desalination. The seawater observed comes from the Southeast Sulawesi Province, Indonesia, which has a good sea salt level, and the surrounding community still has difficulty obtaining clean water for daily use.

2. Material and Methods

2.1. Chemicals and materials

Cellulose acetate (CA, purity, 99%), Polyethylene glycol (PEG 400, purity, 99%), TiO_2 Degussa P25 (Purity: 99%), and 2-Amino-2-deoxy-(1,4)-β-D-glucopyranose, Poly-(1,4-β-D-glucopyranosamine) (chitosan, purity: 70%) were purchased from Sigma-Aldrich. The acetone solution (Purity: 99%) was purchased from Merck & Co., Inc.

2.2. Feed water collection

Seawater samples for testing were collected from Toronipa Beach in Konawe Regency, Southeast Sulawesi Province, Indonesia. This location was chosen due to its popularity as a tourist destination and the ongoing challenges coastal communities face in accessing freshwater [27]. The sampling process was conducted approximately 10 meters from the shoreline. We collected 5 gallons of seawater (equivalent to 5 × 3.78 Liters) and passed it through a filter cloth to eliminate impurities, such as seagrass and sand. The filtered samples were then stored in a sample container at room temperature to maintain their integrity for further laboratory analysis.

2.3. Synthesis of TiO_2-NPs–incorporated Chitosan membranes

In this study, 2 grams of CA and 0.5 grams of PEG were mixed in a 50 mL beaker and followed by adding 2 mL of chitosan and 17 mL of an acetone solvent. The media was stirred constantly at 130°C until homogeneous for 24 h. After obtaining a homogeneous solution, it was printed on a flat glass plate for 15 minutes. The membrane layer dries slightly, followed by TiO_2-NPs colloidal coating according to the coating variation by coating evenly on the membrane surface. The media was allowed to dry for 64 hours in a sterile room. After that, to release the membrane that has dried on the surface of the glass plate, the method is to soak the media in cold water for 15 minutes. The membrane is ready for use in the reverse osmosis method design tool with UV light emission.

2.4. Membrane material characterization

The TiO_2 incorporated in chitosan membranes was characterized to confirm the presence of TiO2 in chitosan membranes. The functional group was confirmed using FTIR spectra (Shimadzu, IR Prestige 21) to identify inorganic materials (Ti-O-Ti). Morphological

analysis was also conducted using Scanning Electron Microscopy (SEM) (FEI, Inspect-S50) to observe the porosity of synthesized membranes, and crystallinity was investigated using X-ray diffraction (XRD, PAN anlytical X'Pert PRO) to determine the crystallinity of a material.

2.5. Reverse osmosis test

The synthesized membranes were assessed for their performance in a desalination process utilizing the reverse osmosis (RO) technique. The portable design of the reverse osmosis pilot instrument (Fig. 1) involves introducing feed water into a storage tank, which is then pumped into a pretreatment system incorporating filtering materials such as sand, palm fibre, stone, and charcoal. Subsequently, seawater is directed into a horizontal tank equipped with vertically positioned synthetic membranes and subjected to UV light exposure. Excess water is returned to the pretreatment process, while the remainder passes through the membranes and is collected in a permeate container. The permeate was subsequently tested to evaluate membrane performance parameters, including salt rejection, water flux, pH, and salinity.

3. Results and Discussion

This study aims to overview the effect of the surface coating method on TiO_2-NPs incorporated chitosan membrane. In Figure 1, we modelled desalination technology engineering to observe the performance of TiO_2-NPs-chitosan membrane in reverse osmosis (RO) system. Schematically, the feed water is flowed and passed through a pretreatment material consisting of activated carbon. A pressurized pump passes the feed water from the pretreatment through the membrane with UV light to see the photocatalyst performance of the membrane containing TiO_2-NPs. The membrane fabrication, characterization, and performance tests were identified to determine the well-oriented performance membrane, such as identifying flux and salinity values.

The synthesized membrane has been fabricated with a coating process using TiO_2-NPs of 0.25 g and 0.50 g. The simple membrane fabrication was conducted by inverse technique, in which the mixed solution was evaporated on a glass plate for 64 h. The organic solution also plays an essential role in accelerating the evaporation process to obtain a high permeability and resistance to hydrophilic properties, making it easily soluble in water [27]. The organic solvent (acetone) was chosen in this study because it is environmentally friendly for plastic, pharmaceutical, and paper fabrication. Moreover, acetone can reduce the boiling point so the membranes can quickly be dried. In this study, the fabricated membranes have been printed with a diameter size of 8 cm, which

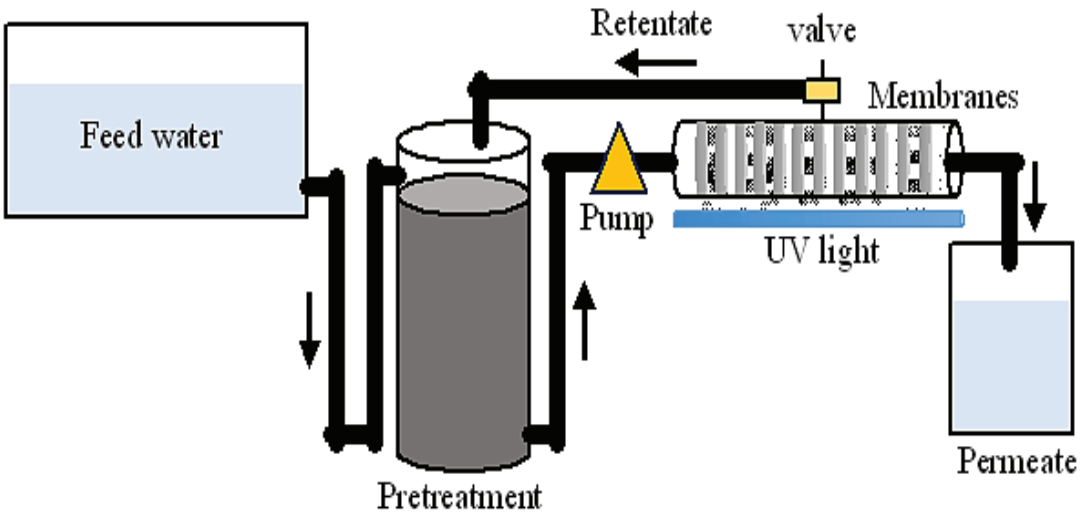

Fig. 1. Schematic of reverse osmosis desalination

helps determine the membrane's performance for water flux. Several studies have also reported that the addition of TiO_2-NPs to organic membranes that have been developed can improve the hydrophilicity and selectivity properties expected for high membrane permeability flux. Herein, we present the fabrication of the chitosan membrane by showing the unique characterization membranes incorporated into TiO_2-NPs using FTIR, SEM, and XRD. They are the basics for material characterization for an overview of a functional group of Ti-O-Ti bonds, morphological analysis of fabricated membranes incorporated TiO_2-NPs and crystallinity. Besides that, performance tests over fabricated membranes were also reported, including salt rejection, water flux, pH, and salinity. All tests will be explained in detail below.

3.1. Membranes characterization

3.1.1. Fourier transform infrared spectroscopy (FTIR)

The identification of functional groups has been applied using FTIR analysis to identify the chemical compound groups presented in the fabricated membranes. Raw material based on CA, PEG, as basic membranes, and chitosan contains organic compounds that are easily identified using FTIR. Meanwhile, the TiO_2-NPs are also placed in fingerprint regions under 750-400 nm [28]. The organic functional group is bonded with -OH stretching affected by water, alcohol specimens, and acidic conditions or organic oxidation. The presence of the -OH group in membranes characterizes the hydrophilicity value over membranes. The polarization functional group from OH attracts the attention of polar groups that bind together in several chemical positions [29]. The hydrophilicity value can be calculated using the peak area from -OH groups in the FTIR graph using the origin application.

Based on Figure 2, the FTIR spectra for each fabricated membrane are shown by varying composition and without adding TiO_2-NPs. The specific absorption on wavenumber of 3479-3549 cm^{-1} is presented of -OH groups from cellulose acetate that have -OH bonds outside the aromatic ring. The C=O (ester) group was presented under the wavenumber of 1755-1757 cm^{-1}, and the -CH group was marked on 2887-2889 cm^{-1}. In addition, the $-CH_3$ group is also shown on 1433-1436 cm^{-1} and the $-NH_2$ group on wavenumber of 1527-1544 cm^{-1}. The Ti-O-Ti group was identified in the specific wavenumber range of 850-500 cm^{-1}, identified with widened absorption.

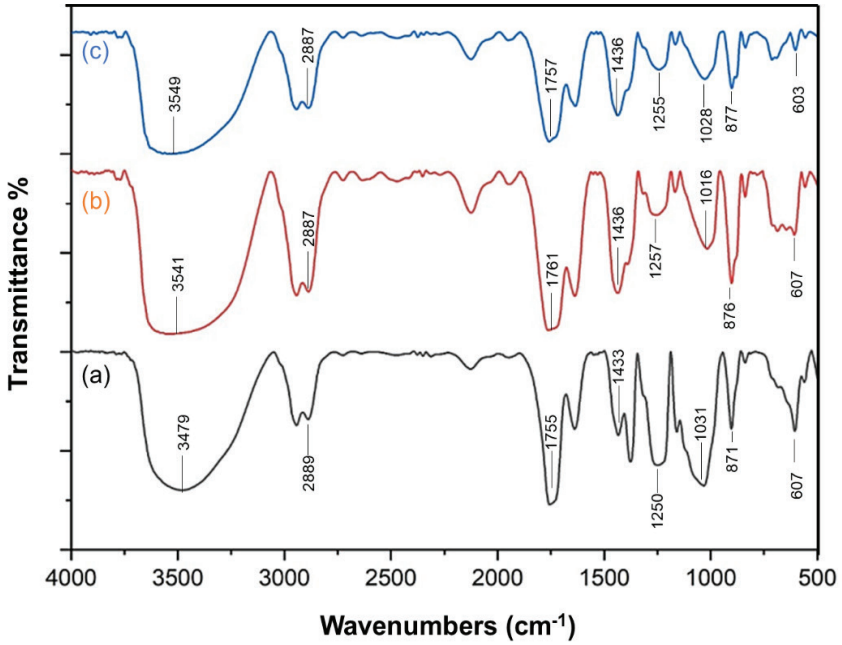

Fig. 2. FTIR spectra of the fabricated membranes, (a) Chitosan polymer membrane, (b) Chitosan–TiO2-NPs (I: 0.25 g), and (c) Chitosan–TiO2-NPs (II: 0.50 g)

Meanwhile, 871-877 cm^{-1} wavenumber indicated a pyranose ring (CA), and 1250-1257 cm^{-1} presented C-O-C stretching from cellulose acetate. Referring to Figure 2, the fabricated membranes have chemically shown -OH, C=O, C-O, -CH $-CH_3$, NH_2, and C-O-C groups. The functional groups -OH, C-O, C=O, and C-O-C are the main functional groups of CA. Particularly, the wavenumber characteristics could be identified, such that the peak area of the -OH group was increased along with the addition of TiO_2-NPs. This condition indicates an increase in hydrophilicity in the fabricated membrane. The highly increased number of hydroxyl groups also plays a role in photocatalyst and hydrophilicity performances. Based on Figure 1, the principle of RO performance against the fabricated membrane is irradiating under UV light for 30 minutes to activate the performance of TiO_2-NPs attached to the membrane surface. In addition, the atomic mass effect of TiO_2-NPs is expressed using Hooke's law equation, where the more significant the mass of interacting atoms indicates, the lower the vibrational frequency to a smaller wavenumber.

3.1.2.Scanning Electron Microscopy (SEM)

SEM identification is frequently used as an analytical method to determine the morphological structure of fabricated membranes. The typical structure on the membrane area illustrates the difference of membrane surface against incorporated TiO_2-NPs. Based on SEM analysis,

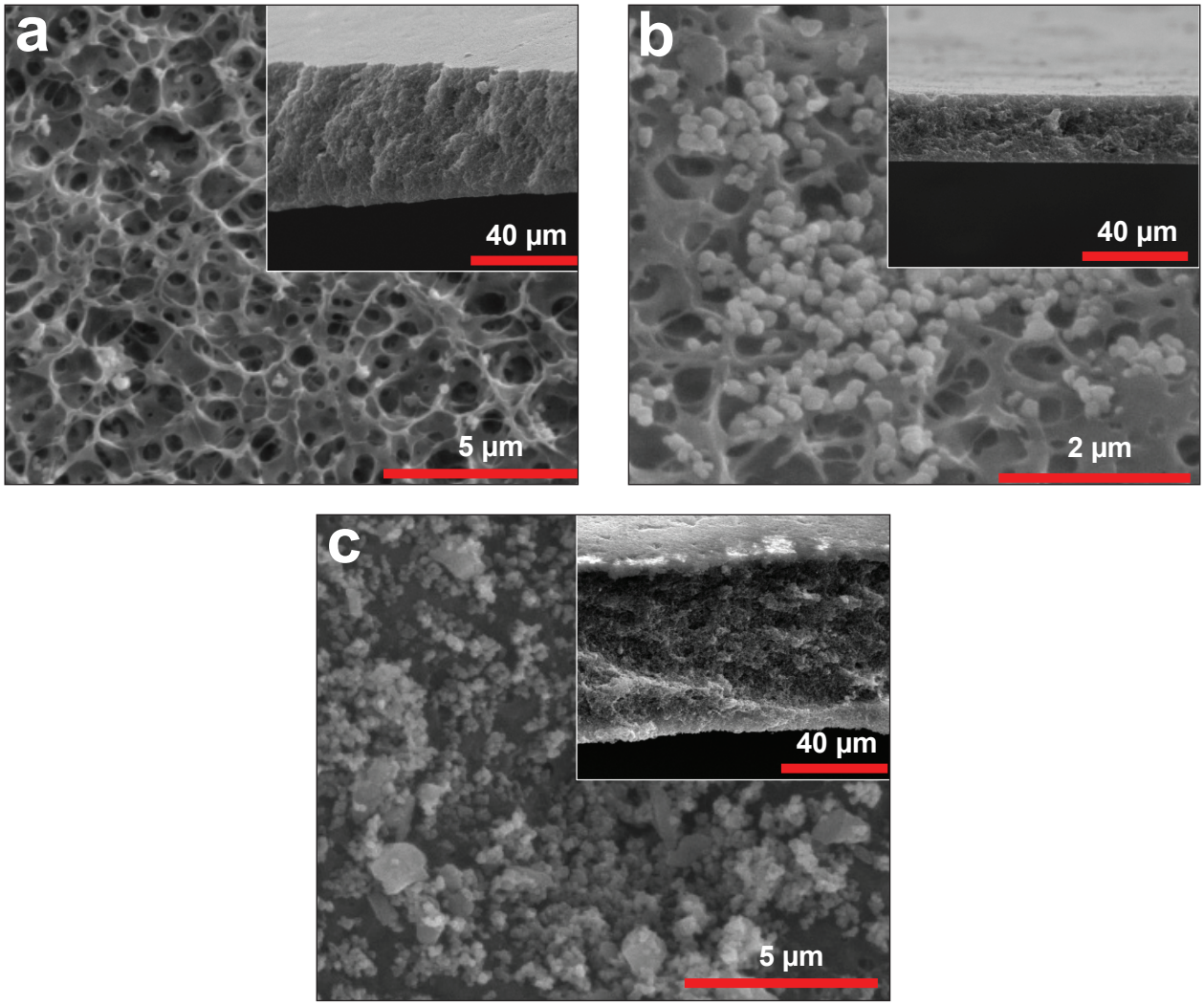

Fig. 3. Morphological analysis of fabricated membranes;
(a) Chitosan polymer membrane [27], (b) Chitosan-TiO_2 (I) (0.25 g), and (c) Chitosan-TiO_2 (II) (0.5 g)

indentations and protrusions of the fracture surface were also generated, and the enlargement of the pores in the fabricated membrane was observed.

Figure 3 shows a typical morphological analysis of the fabricated membrane; it shows the difference in morphological structure between without and the addition of TiO_2-NPs. Figure 3a shows that the variable chitosan polymer membrane without TiO_2-NPs has irregular pores compared to Figures 3b and 3c. The inclusion of TiO_2-NPs is reflected in a reduction in pore size, particularly at higher TiO_2 concentrations. The solvent exchange process influences the formation of membrane pores during membrane synthesis, which facilitates the entry of TiO_2-NPs into the lattice of membrane pores. Additionally, the incorporation of TiO_2-NPs results in a decrease in pore size due to the small particle size of TiO_2, which attracts particles into the membrane pores. PEG also plays a crucial role in standardizing and increasing the number of membrane pores. Using acetone as a solvent leads to a delayed demixing mechanism, creating tighter pores. To assess the pore size distribution of the fabricated membranes, Figure 4 presents our calculations. In Figure 4a, the average pore size is approximately 800 nm; in Figure 4b, it is around 500 nm, and in Figure 4c, it is roughly 200 nm. These peaks represent the average pore size of each membrane. The largest peaks are observed when TiO_2-NPs are not added, while the smallest pore size is seen when 0.5 grams of TiO_2-NPs are added. This aligns with the morphological

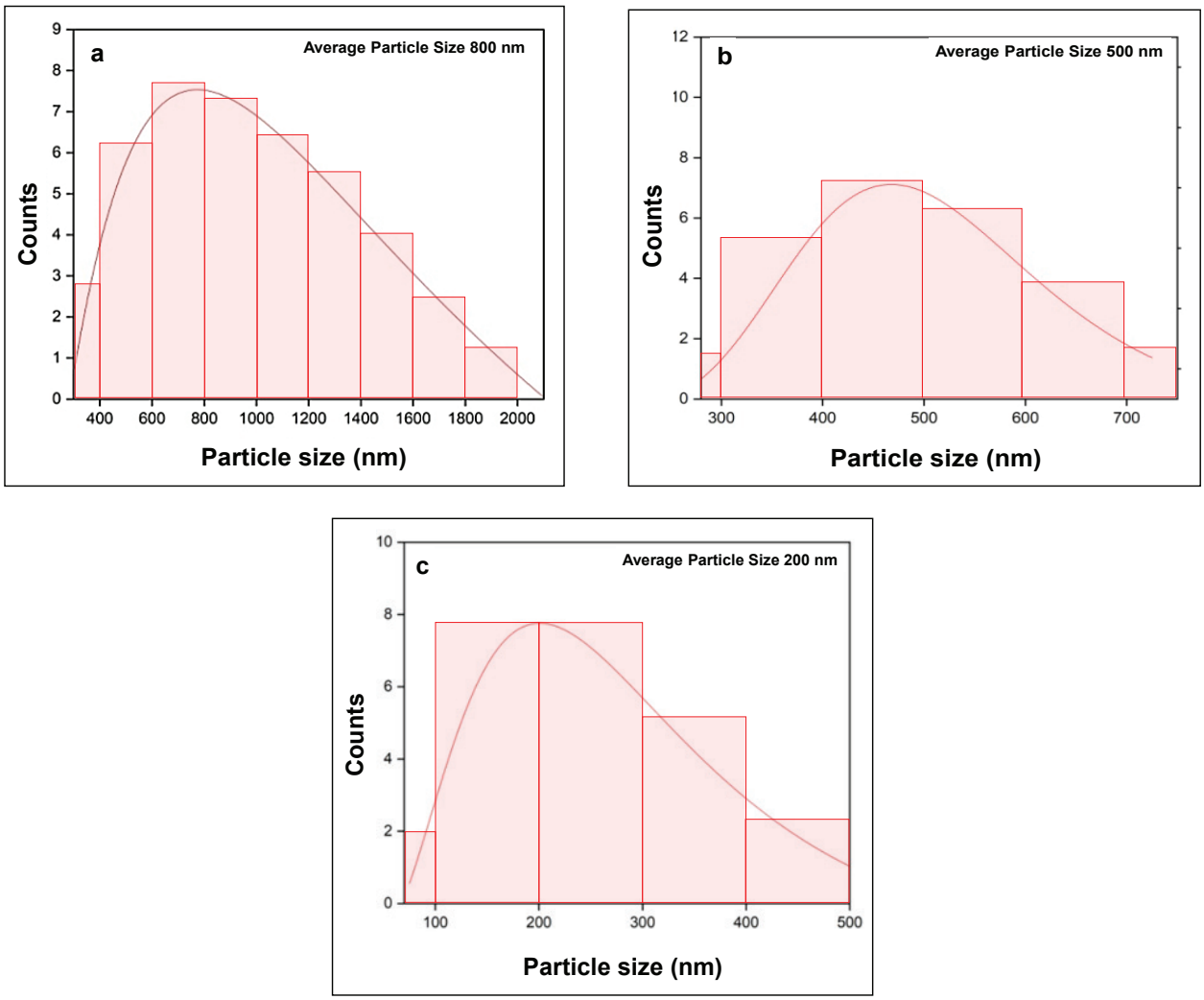

Fig. 4. Histogram of the particle size distribution of fabricated membranes, (a) Chitosan polymer membrane, (b) Chitosan–TiO_2-NPs (I), (c) Chitosan–TiO_2-NPs (II).

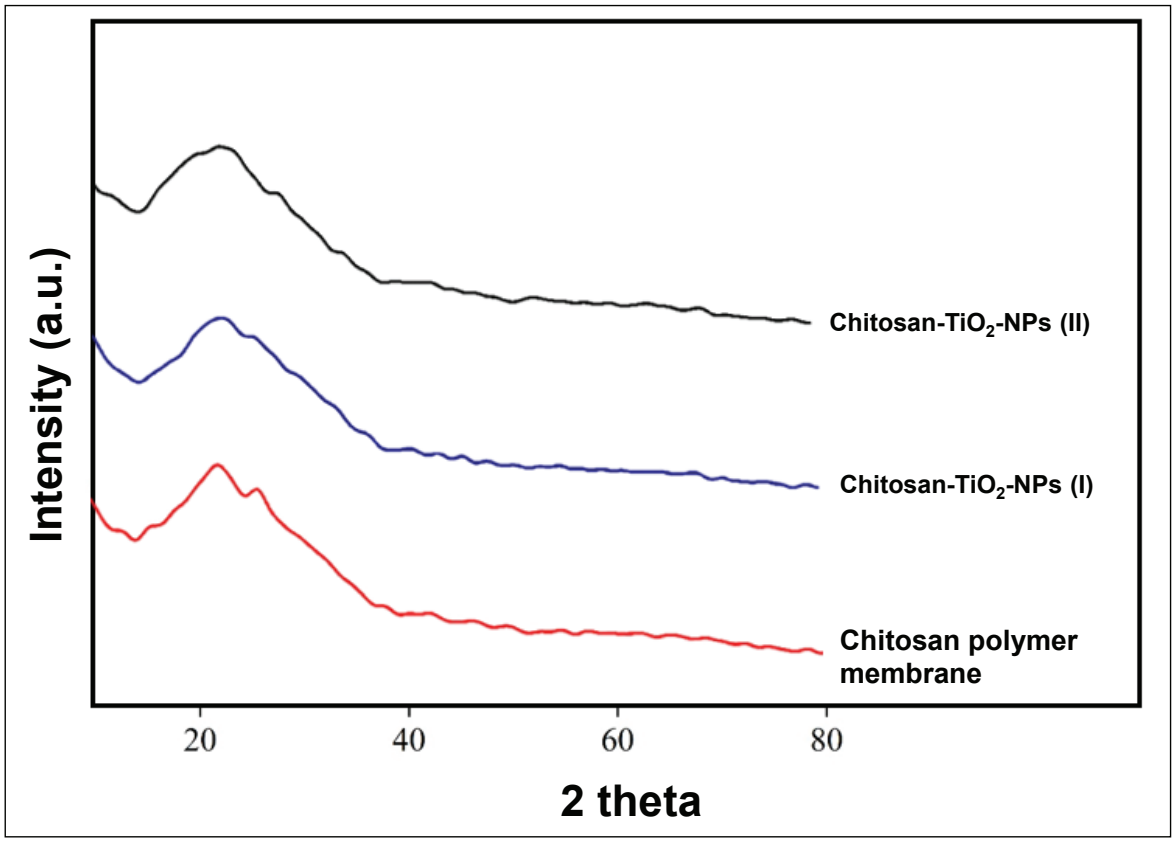

Fig. 5. XRD pattern of fabricated membranes

analysis, indicating that adding TiO_2 further reduces membrane pore size. As per Dietz et al., the typical range of membrane pore sizes formed falls within 100 nm to 10,000 nm, categorizing them as microfiltration membranes [30].

3.1.3. X-ray diffraction (XRD)

The crystallinity phase is also identified to analyze the fabricated membrane, including the composition or type of crystals formed, such as amorphous, semicrystalline, or crystalline. Generally, the TiO_2 phase has three crystals formed: anatase, rutile, and brookite types. In Figure 5, the fabricated membrane includes an amorphous phase with no sharp peaks. High absorption peaks at two theta 25.49° (type I: 0.25 g TiO_2) and 25.84° (type II: 0.50 g TiO_2) correspond to the peaks belonging to the anatase phase based on JCPDS No. 21-1276. The same peak was also shown without adding TiO_2 at two theta of 22.95°. This was identified from the crystallinity of the chitosan polymer membrane. Based on particle size analysis, the average particle size of TiO_2 in chitosan-TiO_2-NPs (I) and chitosan-TiO_2-NPs (II) were 2.92 nm and 2.97 nm, respectively These conditions were expressed that the TiO_2 was quickly inserted into the membrane pore lattice to strengthen the structure and reduce the membrane pores. In addition, a lower crystalline nature or higher amorphous structure coincides with the decrease of polymer chain packing and will result in higher permeability performance.

3.2. Reverse osmosis test

3.2.1.Determination of water flux and salt rejection

Before the analysis of water flux, the water compaction in the RO system was conducted to achieve a uniform structure with steady water flux. This condition has been performed using a high-pressure pump in the RO system to remove the air trapped inside the installation. The compaction of water pressure results in changes in the membrane position. However, the water pressure in this study was 68 bar above an osmosis pressure for

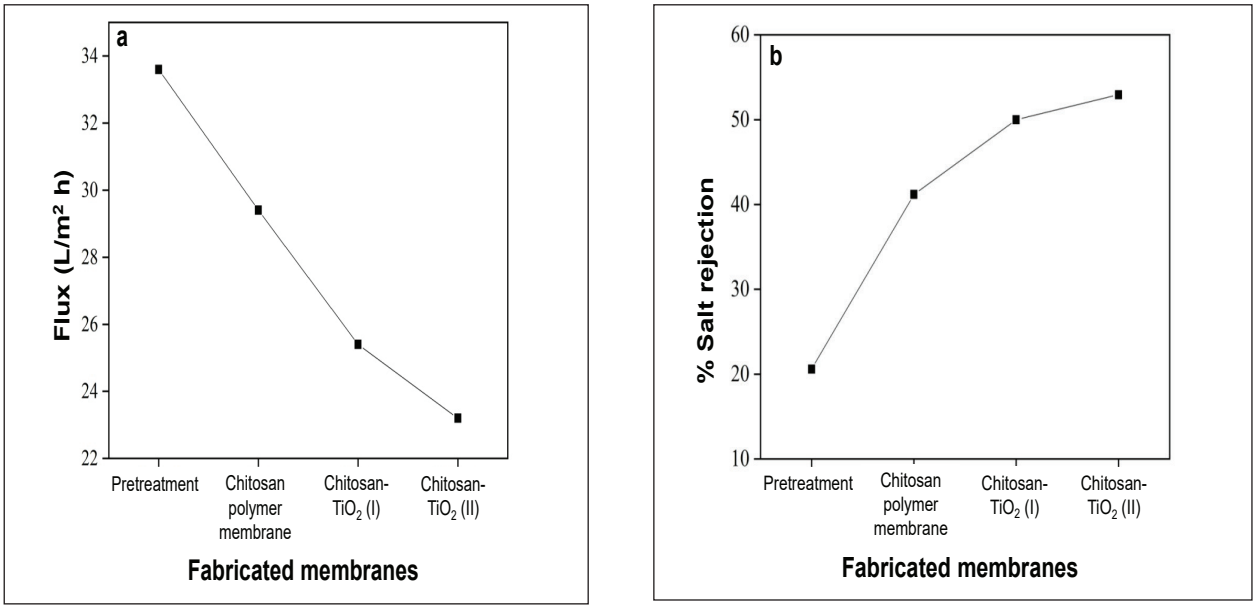

Fig. 6. Membranes performance tests, (a) water flux and (b) salt rejection

60 minutes. The fabricated membrane showed an almost constant decrease with the addition of TiO_2-NPs, and RO testing for 60 min of operation has confirmed that the permeate production is very minimal due to the tiny membrane pores (Fig. 6a). The TiO_2 plays an essential role in the porosity and selectivity of the fabricated membranes, this condition makes the membrane pores tighter. The slow flux reduction can be associated with the porosity and strength of the membrane. The compaction results in a denser membrane structure, which minimizes the water flux.

Salt rejection was also identified to determine the salt content in the permeate. A desalination test was carried out with the RO system by comparing salt concentration results to permeate water with feed water whose units refer to the percentage of salt rejected. Based on the analytical results in Figure 6b, salt rejection increases with the addition of TiO_2-NPs. This graph is inversely proportional to the water flux. It has been discovered that such fine-regulation of the polymer microporous structure leads to a crucial increase in the salt rejection of the chitosan-TiO_2 (II) membrane towards high-performance RO desalination [16]. Based on the salt rejection results, adding 0.5 grams of TiO_2 can increase salt rejection with a value of 52.94% following the morphological analysis that the membrane pore size affects salt rejection in RO desalination.

3.2.2. Determination of pH and salt contents

Water quality (pH) based on chemical properties is also analyzed using a pH meter to determine acidity or alkaline salt content. In general, the pH of seawater varies depending on the location of the collection area, with a range of pH conditions between 6.0 and 8.5. The feed water comes from Southeast Sulawesi Province, Indonesia, with a pH of 7.7. We determined the pH level to observe if the RO desalination process of seawater influences changes in pH value. Fluctuations also affect the high and low pH of the feed water in terms of the levels of O_2 and CO_2 dissolved in the feed water. Based on the analysis results (Figure 7a), the pH measurement results decrease along with the increase in TiO_2 addition to the membrane; although this condition is not too significant, it shows there is little change.

Furthermore, the surface potentials of the membranes produced exhibit negativity when the pH is above 7 and 6. This negativity signifies a substantial electrostatic repulsion between the negatively charged membrane surface and the Cl^- ions at higher pH levels [31]. As a result, the desalination process led to a reduction in salt

levels of over 53%. These findings are consistent with earlier studies that have reported similar data regarding the incorporation of TiO_2 into CA-PEG membranes [31]. The results of salt content by three RO membranes at different TiO2-NP concentrations are shown in Figure 7b. The experiment was conducted using a refractometer instrument to identify the measured salt concentration of the feed water. This was calculated based on the percentage of salt content before and after the RO desalination process. Generally, salinity is defined as the salt content at which the salt level in aqueous solutions and some seawater have unequal salinity values. In this case, the salinity of pure seawater on Southeast Sulawesi beach ranges from 34 ppt. Based on Figure 7b, there is a decrease in salt content in permeate water that passes through each fabricated membrane. The feed water passed the pretreatment process and decreased the salt content to 27 ppt. This indicates that the pretreatment process containing sand, palm fibre, activated charcoal, and filter paper contributes to a decrease in salt content by 20.5%. This was followed by a membrane without TiO_2 addition, which reduced 26% (20 ppt) from the pretreatment process. Furthermore, the performance comparison of the membrane with the addition of TiO_2 0.25 g and 0.5 g showed a decrease in the percentage of salt content by 37% (17 ppt) and 41% (16 ppt), respectively. From the results of this study, it can be concluded that increasing the composition of TiO_2 as an agent of permeability and selectivity of chitosan membrane has a high effect in changing the salt content in seawater.

Numerous research studies imply that TiO_2-NPs alter water flux and rejection performance, as shown in Table 1[27,32-35]. All studies using the phase inversion method (NIPS) and solution casting to fabricate RO membranes incorporated with TiO_2-NPs have produced different flux and salt rejection results. The addition of TiO_2 resulted in an increase in total salt rejection followed by flux values. This condition implies that the TiO_2-modified membrane affects the porosity of the membrane, which also acts the performance. When the average pore size increases, the CA-TiO_2 membrane becomes more porous.

4. Conclusion

The proposed method introduced TiO_2-NPs into chitosan membranes to enhance permeability and selectivity performance for reverse osmosis (RO) desalination. It was incorporated into

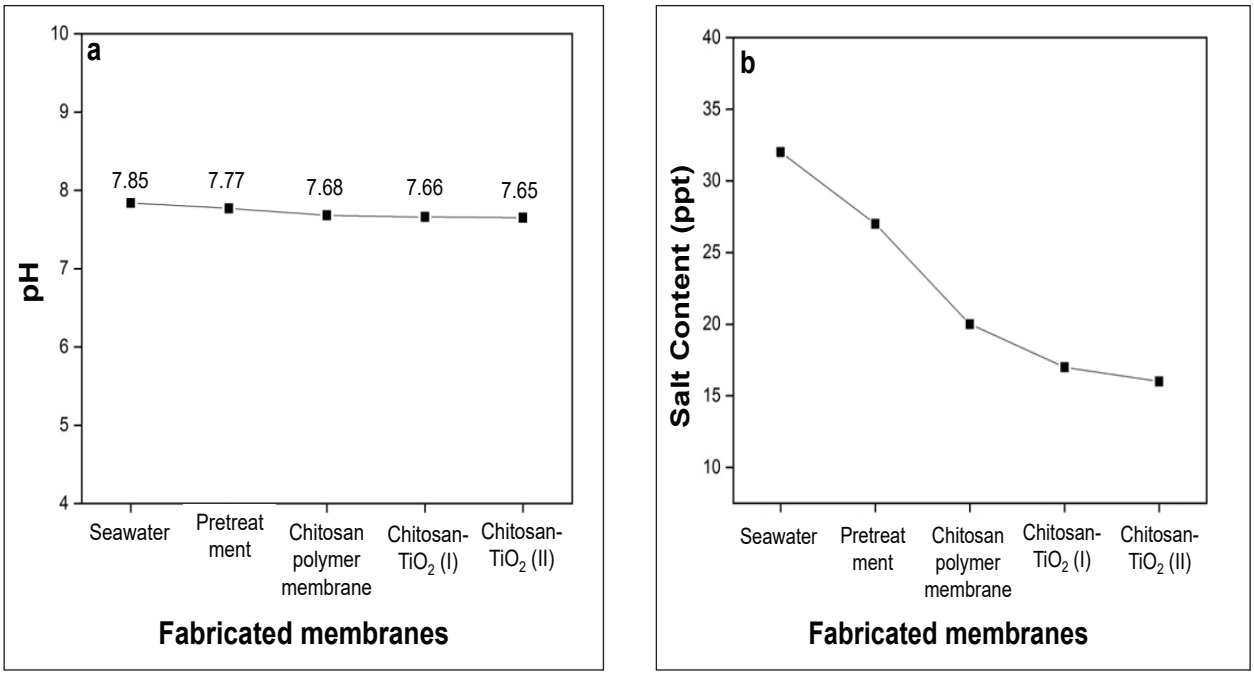

Fig. 7. Membranes performance tests, (a) pH and (b) salt content

Table 1. Comparison between previous and current studies

Polymer composition	NPs	Methods	Flux (LMH)	Pollutant	Rejection %	Ref.
Cellulose acetate / polyethylene-glycol / chitosan	TiO_2	Phase inversion method (NIPS) and casting solution	50.00	Salt	61.76	[27]
Polyvinyl alcohol / cellulose acetate	TiO_2	Phase inversion method (NIPS) and casting solution	15.50	Salt	92	[32]
Cellulose acetate	TiO_2	Phase inversion method (NIPS) and casting solution	58.21	Salt	92.6	[33]
Polyvinylpyrrolidone / N-methyl pyrrolidone	TiO_2	Phase inversion method (NIPS) and casting solution	34.3	Salt	-	[34]
Polyamide/carbon dots	TiO_2	Phase inversion method (NIPS) and casting solution	54.6	Salt	99.2	[35]
Chitosan/cellulose acetate / polyethylene-glycol	TiO_2	Phase inversion method (NIPS) and casting solution	23	Salt	52.94	This work

chitosan membranes using the surface coating method, with varying TiO_2 mass fractions of 0.25 grams and 0.50 grams. The physical characterization of the fabricated membranes revealed functional groups representing organic and inorganic compounds. Additionally, TiO_2-NPs were identified within the wavenumber range of 850-500 cm^{-1}, indicating the presence of Ti-O-Ti bonds. Morphological analysis exhibits the TiO_2-NPs led to significantly smaller pores in chitosan membranes due to their contribution to the amorphous phase structure. During the RO desalination process, the performance of the fabricated membranes was assessed in terms of water flux and salt rejection. The addition of TiO_2-NPs resulted in a 23 $Lm^{-2}\,h^{-1}$ decrease in water flux and a 52.94% increase in salt rejection. Furthermore, the pH and salt content values were measured, indicating a reduction under favourable conditions. TiO_2 played a crucial role as a permeability and selectivity enhancer within the TiO_2-chitosan membranes, significantly reducing salt content in seawater.

5. Acknowledgments

Financial support from the Ministry of Education, Culture, Research, and Technology, Republic of Indonesia, is gratefully acknowledged for basic research grant no. 51/UN29.20/PG/2023 and World Class Professor research grant no. 3252/E4/DT.04.03/2023. Department of Chemistry, Faculty of Mathematics and Natural Sciences, Halu Oleo University, and Photocatalysis Laboratory for facilitating this research.

6. References

[1] P.H. Nienhuis, J. Coosen, W. Kiswara, Community structure and biomass distribution of seagrasses and macrofauna in the Flores Sea, Indonesia, Netherlands J. Sea Res., 23 (1989) 197–214. https://doi.org/10.1016/0077-7579(89)90014-8.

[2] E. Hastuti, M.W. Wardiha, A study of brackish water membrane with ultrafiltration pretreatment in indonesia's coastal area, J. Urban Environ. Eng., 6 (2012) 10–17. https://doi.org/10.4090/juee.2012.v6n1.010017.

[3] S. Han, Y.-W. Rhee, S.-P. Kang, Investigation of salt removal using cyclopentane hydrate formation and washing treatment for seawater desalination, Desalination, 404 (2017) 132–137. https://doi.org/10.1016/j.desal.2016.11.016.

[4] S. Timoori, Environmental Health: Evaluation of heavy metals pollution in Isfahan industrial zone from soils, well/eluent waters and waste water by microwave-electro-thermal atomic absorption spectrometry, Anal. Methods Environ. Chem. J., 2 (2019) 55–62. https://doi.org/10.24200/amecj.v2.i01.44.

[5] B. Suhartawan, J. Haurissa, S.A. Rumawak, Lake Sentani water quality index based on NSF-WQI as raw water for drinking water for Lake Sentani Coastal communities, Jayapura Regency, J. Syntax Admiration, 3 (2022) 1189–1204. https://doi.org/10.46799/jsa.v3i9.481.

[6] K. Katsanou, H.K. Karapanagioti, Surface water and groundwater sources for drinking water, Appl. Adv. Oxid. Process. Drink. Water Treat., (2019) 1–19. https://doi.org/10.1007/698_2017_140.

[7] S.H. Mutasher, H.S. Al-Lami, Preparation of chitosan films plasticized by lauric and maleic acids, Anal. Methods Environ. Chem. J., 5 (2022) 43–54. https://doi.org/10.24200/amecj.v5.i04.209.

[8] Y. Cai, J. Wu, S.Q. Shi, J. Li, K.-H. Kim, Advances in desalination technology and its environmental and economic assessment, J. Clean. Prod., 397 (2023) 136498. https://doi.org/10.1016/j.jclepro.2023.136498.

[9] A.M. Ghaithan, A. Mohammed, L. Hadidi, Assessment of integrating solar energy with reverse osmosis desalination, Sustain. Energy Technol. Assessments, 53 (2022) 102740. https://doi.org/10.1016/j.seta.2022.102740.

[10] A. Hassanzadeh, B. Amirheidari, A. Salarifar, A. Asadipour, Y. Pourshojaei, Synthesis and identification of meta-(4-bromobenzyloxy) benzaldehyde thiosemicarbazone (MBBOTSC) as novel ligand for cadmium extraction by ultrasound assisted-dispersive-ionic liquid-liquid micro extraction method, Anal. Methods Environ. Chem. J., 4 (2021) 92–106. https://doi.org/10.24200/amecj.v4.i04.161.

[11] A.B.D.N. Kurnia, R. Ismiati, A. Annisa, F. Finandia, N.N.A. Nissa, R.C. Dewi, Economic evaluation analysis of nano-silica ultrafiltration membrane production from sand, Int. J. Energ., 3 (2018) 6–9. https://doi.org/10.47238/ijeca.v3i1.59.

[12] A. Knebel, J. Caro, Metal–organic frameworks and covalent organic frameworks as disruptive membrane materials for energy-efficient gas separation, Nat. Nanotechnol., 17 (2022) 911–923. https://doi.org/10.1038/s41565-022-01168-3.

[13] V. Vatanpour, M.E. Pasaoglu, H. Barzegar, O.O. Teber, R. Kaya, M. Bastug, A. Khataee, I. Koyuncu, Cellulose acetate in fabrication of polymeric membranes: A review, Chemosphere, 295 (2022) 133914. https://doi.org/10.1016/j.chemosphere.2022.133914.

[14] I. Ounifi, Y. Guesmi, C. Ursino, R. Castro-Muñoz, H. Agougui, M. Jabli, A. Hafiane, A. Figoli, E. Ferjani, Synthesis and characterization of a thin-film composite nanofiltration membrane based on polyamide-cellulose acetate: application for water purification, J. Polym. Environ., 30 (2022) 707–718. https://doi.org/10.1007/s10924-021-02233-z

[15] Y. Yamashita, T. Endo, Deterioration behavior of cellulose acetate films in acidic or basic aqueous solutions, J. Appl. Polym. Sci., 91 (2004) 3354–3361. https://doi.org/10.1002/app.13547.

[16] Y. Yang, Z. Wang, Z. Song, D. Liu, J. Zhang, L. Guo, W. Fang, J. Jin, Thermal treated amidoxime modified polymer of intrinsic microporosity (AOPIM-1) membranes for high permselectivity reverse osmosis desalination, Desalination, 551 (2023) 116413. https://doi.org/10.1016/j.desal.2023.116413.

[17] S. Yang, R. Tang, Y. Dai, T. Wang, Z. Zeng,

L. Zhang, Fabrication of cellulose acetate membrane with advanced ultrafiltration performances and antibacterial properties by blending with HKUSt-1@ LCNFs, Sep. Purif. Technol., 279 (2021) 119524. https://doi.org/10.1016/j.seppur.2021.119524.

[18] S. Hasheminasab, J. Barzin, R. Dehghan, High-performance hemodialysis membrane: Influence of polyethylene glycol and polyvinylpyrrolidone in the polyethersulfone membrane, J. Membr. Sci. Res., 6 (2020) 438–448. https://doi.org/10.22079/JMSR.2020.128323.1391.

[19] L. Qi, R. Liang, T. Jiang, W. Qin, Anti-fouling polymeric membrane ion-selective electrodes, TrAC Trends Anal. Chem., 150 (2022) 116572. https://doi.org/10.1016/j.trac.2022.116572.

[20] M. Chaudhary, A. Maiti, Fe–Al–Mn@ chitosan based metal oxides blended cellulose acetate mixed matrix membrane for fluoride decontamination from water: removal mechanisms and antibacterial behavior, J. Memb. Sci., 611 (2020) 118372. https://doi.org/10.1016/j.memsci.2020.118372.

[21] P.S. Bakshi, D. Selvakumar, K. Kadirvelu, N.S. Kumar, Chitosan as an environment friendly biomaterial–a review on recent modifications and applications, Int. J. Biol. Macromol., 150 (2020) 1072–1083. https://doi.org/10.1016/j.ijbiomac.2019.10.113.

[22] M. Nurdin, D. Wibowo, T. Azis, R.A. Safitri, M. Maulidiyah, A. Mahmud, F. Mustapa, R. Ruslan, A. Salim, L. Ode, Photoelectrocatalysis response with synthetic Mn–N–TiO2/Ti electrode for removal of rhodamine B dye, Surf. Eng. Appl. Electrochem., 58 (2022) 125–134. https://doi.org/10.3103/S1068375522020077.

[23] D. Wibowo, M.Z. Muzakkar, M. Maulidiyah, M. Nurdin, S.K.M. Saad, A.A. Umar, Morphological analysis of Ag doped on TiO2/Ti prepared via anodizing and thermal oxidation methods, Biointerface Res. Appl. Chem., 12 (2022) 1421–1437. https://doi.org/10.33263/BRIAC122.14211427.

[24] M. Natsir, M. Maulidiyah, A. Ansharullah, Z. Arham, D. Wibowo, M. Nurdin, Natural biopesticide preparation as antimicrobial material based on lignin photodegradation using mineral ilmenite (FeoTio2), Int. Res. J. Pharm., 9 (2018) 170–174. https://doi.org/10.7897/2230-8407.096111.

[25] M. Nurdin, N. Dali, I. Irwan, M. Maulidiyah, Z. Arham, R. Ruslan, B. Hamzah, S. Sarjuna, D. Wibowo, Selectivity determination of Pb2+ Ion based on TiO2-Ionophores BEK6 as carbon paste electrode composite, Anal. Bioanal. Electrochem., 10 (2018) 1538–1547. https://doi.org/-.

[26] D. Wibowo, M.Z. Muzakkar, S.K.M. Saad, F. Mustapa, M. Maulidiyah, M. Nurdin, A.A. Umar, Enhanced visible light-driven photocatalytic degradation supported by Au-TiO<inf>2</inf> coral-needle nanoparticles, J. Photochem. Photobiol. A Chem., 398 (2020) 112589. https://doi.org/10.1016/j.jphotochem.2020.112589.

[27] D. Wibowo, F. Mustapa, S. Selviantori, M. Idris, A. Mahmud, M. Maulidiyah, M.Z. Muzakkar, A.A. Umar, M. Nurdin, CA/PEG/Chitosan membrane incorporated with TiO2 nanoparticles for strengthening and permselectivity membrane for reverse osmosis desalination, Environ. Nanotechnol. Monit. Manag., 20 (2023) 100848. https://doi.org/10.1016/j.enmm.2023.100848.

[28] S. Chelbi, D. Djouadi, A. Chelouche, L. Hammiche, T. Touam, A. Doghmane, Effects of Ti-precursor concentration and annealing temperature on structural and morphological properties of TiO 2 nano-aerogels synthesized in supercritical ethanol, SN Appl. Sci., 2 (2020) 1–10. https://doi.org/10.1007/s42452-020-2633-3.

[29] Y.-H. Chiao, A. Sengupta, S.-T. Chen, S.-H. Huang, C.-C. Hu, W.-S. Hung, Y. Chang, X. Qian, S.R. Wickramasinghe, K.-R. Lee, Zwitterion augmented polyamide membrane for improved forward osmosis performance with significant antifouling characteristics,

Sep. Purif. Technol., 212 (2019) 316–325. https://doi.org/10.1016/j.seppur.2018.09.079.

[30] P. Dietz, P.K. Hansma, O. Inacker, H.-D. Lehmann, K.-H. Herrmann, Surface pore structures of micro-and ultrafiltration membranes imaged with the atomic force microscope, J. Memb. Sci., 65 (1992) 101–111. https://doi.org/10.1016/0376-7388(92)87057-5.

[31] M.H. Oo, L. Song, Effect of pH and ionic strength on boron removal by RO membranes, Desalination, 246 (2009) 605–612. https://doi.org/10.1016/j.desal.2008.06.025.

[32] E.S. Mansor, H. Abdallah, A.M. Shaban, Development of TiO2/polyvinyl alcohol-cellulose acetate nanocomposite reverse osmosis membrane for groundwater-surface water interfaces purification, Mater. Sci. Eng. B, 289 (2023) 116222. https://doi.org/10.1016/j.mseb.2022.116222.

[33] H. Jain, A.K. Verma, R. Dhupper, S. Wadhwa, M.C. Garg, Development of CA-TiO2-incorporated thin-film nanocomposite forward osmosis membrane for enhanced water flux and salt rejection, Int. J. Environ. Sci. Technol., 19 (2022) 5387–5400. https://doi.org/10.1007/s13762-021-03415-x.

[34] A.H. Konsowa, H.Z. AbdAllah, S. Nosier, M.G. Eloffy, Thin-film nanocomposite forward osmosis membrane for water desalination: synthesis, characterization and performance improvement, Water Qual. Res. J., 57 (2022) 72–90. https://doi.org/10.2166/wqrj.2022.034.

[35] V. Vatanpour, S. Paziresh, S.A.N. Mehrabani, S. Feizpoor, A. Habibi-Yangjeh, I. Koyuncu, TiO2/CDs modified thin-film nanocomposite polyamide membrane for simultaneous enhancement of antifouling and chlorine-resistance performance, Desalination, 525 (2022) 115506. https://doi.org/10.1016/j.desal.2021.115506.